3D HEPG2 CELL-BASED CELL TRANSFORMATION ASSAY

Raquel Martín Levy

Recetox, Faculty of Science, Masaryk University, Brno, Czech Republic

Supervisor: Iva Sovadinová

Trabajo de Fin de Grado; 4ºA Biomedicina

Universidad Francisco de Vitoria

Abbreviations

- µL: microlitres.
- 2D: two dimensional.
- 3D: three dimensional.
- 3-MC: 3-methylcholanthrene.
- 3R: Reduce, Replace and Refine.
- AR: aspect ratio.
- CTA: cell transformation assay.
- DMSO: dimethyl sulfoxide
- ECM: extracelullar matrix.
- EtOH: ethanol
- HCC: hepatocellular carcinoma.
- mL: millilitres.
- NC: negative control
- OECD: Economic Co-operation and Development.
- PAHS: polycyclic aromatic hydrocarbons.
- PBS: Buffered Saline solution.
- PHH**:** human primary human hepatocytes.
- SC: solvent control.
- TPA: phorbol ester 12-O-tetradecanoylphorbol-13- acetate.

Index

Abstract

Monolayer *in vitro* cultures of hepatic cells, so-called two-dimensional (2D) liver models do not adequately mimic the natural cell microenvironment because of the lack of different biological features and functions such as cell-to-cell and cell-to-matrix interactions. That is why there is a need to develop and improve three-dimensional (3D) hepatic cell (liver) models, characterized by higher expression of liver cell markers and cell interactions, although they still present some limitations and special requirements.

This study aims to optimize and adapt 3D HepG2 cell-based transformation assay applicable for biomedicine, carcinogenicity research and toxicology. Within the proposed protocol, HepG2 cells spheroids were first exposed to an initiator (3-methylcholanthrene, 3-MC) followed by the exposure to promotor (12-O-tetradecanoylphorbol-13- acetate, TPA) to create a tumor environment and characterize a new hepatocellular carcinoma *in vitro* model. The spheroids were monitored within a culture with a non-destructive and non-invasive bright field microscopy-based assay. The analysis is suitable with manual high-speed automated microscopic image acquisition and automated analysis using an in-house built macro 'Spheroid_Finder' in Fiji/ImageJ software. This protocol was essential to characterize and quantify 3D spheroid formation, size and shape.

The results show that spheroids treated with solvent controls did not differ from non-treated spheroids in size or shape. Interestingly, the spheroids treated with 3-MC alone and with the combination with TPA were smaller than the control spheroids, and their shape and compactness were also affected. On the other hand, spheroids treated with TPA alone were mildly bigger than the control ones, and their shape and compactness were changed. It should be emphasized that to confirm cell transformation, the gene expression related to neoplastic and hepatocellular carcinoma-derived cell lines phenotypes will be further evaluated with RT-qPCR, as well as spheroids functionality by measuring albumin, urea or lactate in the collected medium. Despite this assay needing further optimization and validation to confirm its potential, we conclude that CTA assay utilizing HepG2 3D spheroids can be a promising tool for screening carcinogenicity potential of chemicals or new anti-cancer in biomedical, pharmacological, and toxicological research.

Introduction

Cancer has become a significant public health concern, being worldwide the second leading cause of morbidity and mortality after cardiovascular diseases. Cancer's incidence and prevalence rates are high, and they keep increasing, being responsible in 2020 for 19 million new cases and 9 million deaths (1).

While cancers can not be completely avoided, evidence strongly suggests that susceptibility to the disease can be curbed significantly by reducing the impact of several risk factors. Different interrelated causes can contribute to high cancer incidence as biological agents such as viral and bacterial infections, exposure to synthetic chemicals through work or consumer products, and lifestyle factors such as exposure to sunlight, poor diet, being overweight, and tobacco and/or alcohol consumption. On the other hand, we need to be conscious of family history and ageing, representing unavoidable risk factors (2). These risk factors are reported to collectively contribute to the development of 70–95% of all cancers (3,4).

Chemicals are part of our daily life. When properly used, chemicals significantly contribute to improving our quality of life, health and well-being. Otherwise, some chemicals are highly hazardous and can negatively affect our health and environment when they are improperly managed (4,5,6). The cancer incidence attributable to exposure to toxic chemicals has been estimated to be between 1% and 19% (3). There are many variables to consider in chemically induced carcinogenesis, including duration of exposure, demography, geography, environment, and individual susceptibility (3).

The exogenous chemicals that cause cancer are known as a **carcinogen**, and they are responsible for **carcinogenesis**, a process that occurs when normal cells are transformed into cancer cells (7). Chemical carcinogens can be classified into three main groups (8,9):

- **Ultimate carcinogens** are chemicals with a direct action whose structure confers them the capacity to induce cancer without a previous metabolic activation in the host organism.

- **Procarcinogens,** are chemicals that only become active after a previous metabolic activation to ultimate carcinogens.

- **Co-carcinogens**, are chemical substances that can not induce cancer when administered alone but can enhance the carcinogenic effect of other substances.

Carcinogenesis is recognized as a multipath process in which distinct molecular and cellular alterations occur, consisting of separate but closely linked stages of **initiation**, **promotion**, and **progression** (**Figure 1**) (5,10,11):

- The **initiation** process involves the appearance of mutation or alteration of genes, that might arise spontaneously or induced by exposure to a carcinogenic agent. This initiation can lead to dysregulation of biochemical and cellular signalling pathways associated with cell proliferation, survival, and differentiation. It can be influenced by several factors, such as the rate and type of carcinogenic metabolism and the response of the DNA repair function.

- The **promotion** stage is a process in which actively proliferating preneoplastic cells accumulate. It is a relatively lengthy and reversible process.

- **Progression** is the final stage of neoplastic transformation, between a premalignant lesion and the development of invasive cancer. In this phase, genetic and phenotypic changes, as well as cell proliferation, finally occur. Progression involves a rapid increase in the tumor size, where the cells may undergo further mutations with invasive and metastatic potential.

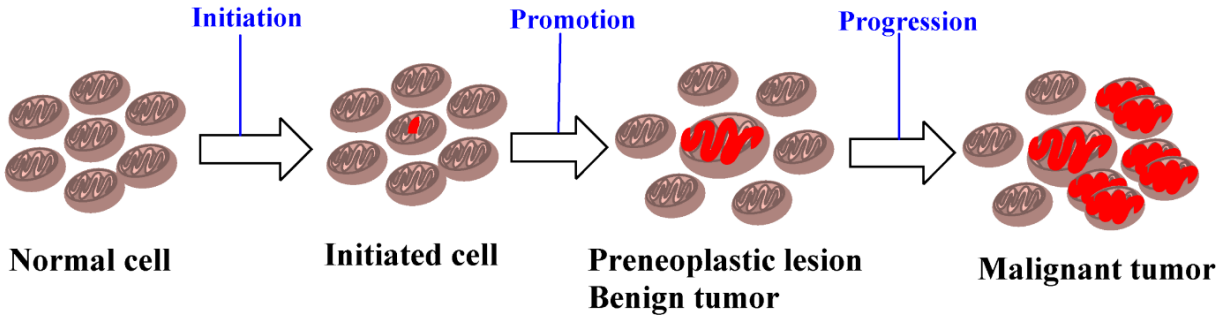

Figure 1. A brief description of initiation, promotion, and progression in the carcinogenesis process. Adapted from Basu A, 2018 (12).

Depending on the chemical structure and mechanisms, carcinogens can be classified as **initiating (genotoxic) agents** or **promoting (non-genotoxic) agents**, with several fundamental differences (12):

- After repeated exposure to initiating agent in a small dosage or a single large exposure leads to carcinogenesis, in contrast to promoting agents, which are not carcinogenic alone.

- An initiating carcinogen is irreversible and additive, whereas the effect of a promoting agent is reversible at the early stages.

- An initiating agent is mutagenic and binds to cellular macromolecules such as DNA, while there is no evidence of covalent binding by a promoting agent (promoting agents are not mutagens).

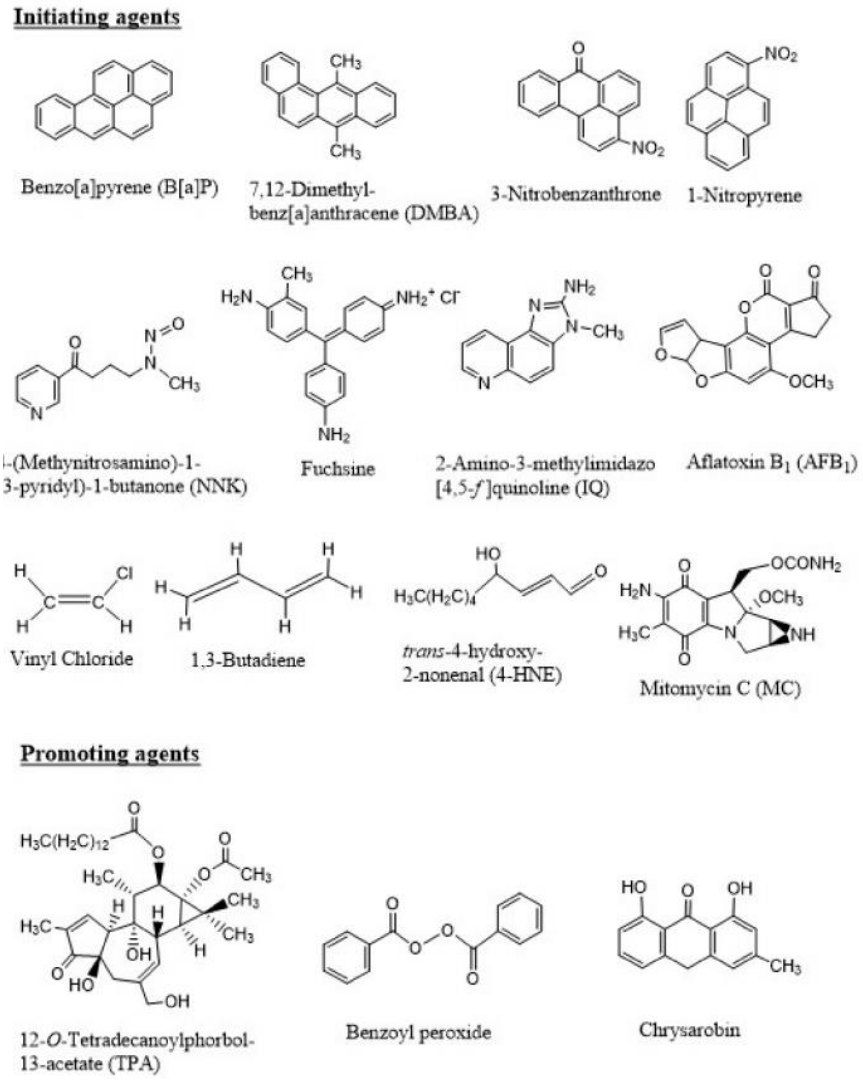

Figure 2. Chemical structures of typical initiating and promoting agents. Adapted from Basu A, 2018 (12).

Initiating agents are structurally different chemicals, including polycyclic aromatic hydrocarbons (PAHs) such as benzo[a]pyrene or 7,12-dimethyl-benz[a]anthracene agents, nitroaromatic compounds, tobacco-specific nitrosamines, fuchsine (a magenta dye), aromatic amines usually formed during the cooking of meat, a naturally occurring molecule produced by *Aspergillus flavus* find in contaminated food (aflatoxin B1) and industrial chemicals (e.g., vinyl chloride; **Figure 2**). The **promoting** agents include for example 12-O-tetradecanoylphorbol-13-acetate, benzoyl peroxide, and chrysarobin (12) (**Figure 2**).

Traditionally, **carcinogenicity bioassays** evaluating the carcinogenic potential of chemicals require animals. However, animal studies have ethical, practical, and economic limitations, due to their high cost, long time for it to be performed and many animals required (13). Nowadays, for toxicology studies, the European Union has promoted the development of different methods, as an alternative to *in vivo* models to succeed implementing the 3R principles (Reduce, Refine, and Replace) (14). The 3R principles and the revolution in 21st toxicology (15) demands an urgent need for advanced development of efficient *in vitro* models for the safety assessment, including two-dimensional (2D) and three-dimensional (3D) *in vitro* cell models (**Figure 3**).

2D cell culture models or monolayer *in vitro* cultures of mammalian adherent cells are characterized by the growth of the cells in a simple, flat monolayer, which is attached to the stiff, typically plastic, surface (16). They have been traditionally used for studying the adverse effects of chemicals and consumer products, including assessing the carcinogenic potential of chemicals using cell transformation assays (CTAs). The 2D CTAs use different cell types such as the Syrian Hamster embryo cells (SHE), liver progenitor WB F344 cells, embryonic mouse fibroblasts BALB/c 3T or Bhas 42 cells, which were established by transfection of BALB/c 3T3 cells with v-Ha-ras (14,17,18,19). The principle of CTAs is to evaluate the effects of chemicals on the growth of specific cell types and their potential progression through a transformation process from being normal cells to fully malignant cells. Experimental protocols include the exposure of 2D monolayer to an initiator (e.g., benzo[a]pyrene or 3-MC) followed by the exposure to a promotor (e.g., TPA), and an easily detectable endpoint is counting malignant foci of transformed cells. However, the validation performance of CTAs was not considered to be sufficiently robust for regulatory test guideline purposes at the Organisation for Economic Co-operation and Development (OECD) (14).

In general, 2D cell culture models are prone to give misleading results because they do not adequately mimic the natural cell microenvironment. The main drawback of 2D models is the lack of biological functions due to limited cell-to-cell and cell-to-extracellular matrix (ECM) interactions (20). Referring to **2D hepatic models**, these result in decreased cell differentiation, modified cell signalling pathways, and a reduced expression and activity of several hepatic enzymes, as CYP450, implicated in the metabolism of xenobiotic substances (phase I and II enzymes) (21). The liver is the primary organ responsible for drug metabolism. In particular, the effects of chemicals and drugs depends on their liver bioactivation and hepatocellular uptake can be misrepresented, as activities of biotransformation enzymes and membrane transporters decrease in monolayer cultures, along with other hepatocyte-specific functions (16,22). These limitations lead to the development of new alternatives to 2D hepatic cell culture.

In contrast, newly developed **3D cell culture models** (**Figure 3**) provide an attractive alternative better reflecting *in vivo* physiology or pathophysiology (23,24). Specifically, 3D hepatic (liver) cell culture models present better cell-cell and cell-ECM interactions and a higher level of liver-specific functions, including metabolic enzyme activities as well as cell morphology and biochemical properties, which reflect *in vivo* conditions more accurately (20). In addition, it was found that 3D liver culture systems:

- Counteract de-differentiation and progressive loss of hepatocellular characteristics of primary hepatocytes *in vitro*.

- Improve liver-specific functions of permanent hepatocellular carcinoma (HCC) derived cell lines (such as HepG2).

- Stimulate hepatic differentiation of human pluripotent stem cells, adult stem cells or progenitor cells (16).

Many 3D cell culture models exist, often categorized as **scaffold-based models**, **scaffold-free models**, or **specialized 3D culture platforms** as microfluidic devices (e.g., organ-on-chips) or micropatterned plates with ECM components (**Figure 3**). Each type has its advantages and disadvantages (25), and it is important to choose the most appropriate 3D cell culture model for a specific application (26).

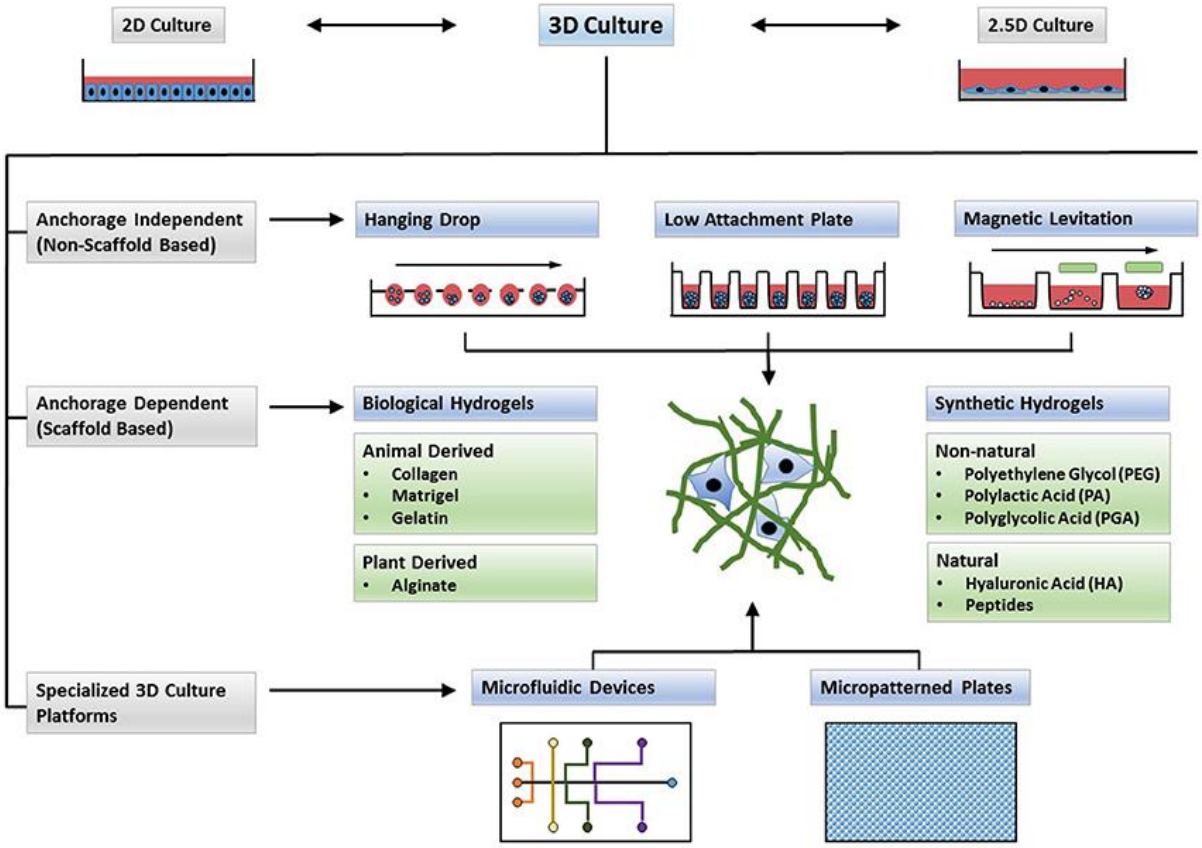

Figure 3. Classification of *in vitro* tissue models and their examples. Adapted from Langhans SA, 2018 (26).

Because a **scaffold-free 3D liver spheroid model** was used in the practical part of the project, this type of 3D model will be described more deeply. **Multicellular spheroids** are a type of scaffold-free 3D models. They are large cell spheres, formed by the spontaneous tendency of cells to aggregate, without using an exogenous scaffold or matrix to support the cells (27). The **multicellular spheroid formation involves** three critical steps (28). First, dispersed cells initially are drawn closer to form loose aggregates. Then, direct cell-cell contact starts to be more and more intensive. Finally (after several days), cells are compacted into solid aggregates and form compact multicellular spheroids. The initial cell suspension seeded is going to determine the size of spheroids. The big advantage of multicellular spheroids is their simple spherical geometry allowing easier modelling of dynamic processes, such as drugs diffusion and cell invasion and angiogenesis due to its characteristics as well-established small tumor model in clinical research (27,29).

Multicellular spheroids mimic physiological characteristics of tissues or tumors regarding cell-cell contact, and ECM-cell contacts, due to their intensive cell-cell interaction and their capacity to synthesize their own ECM, allowing natural cell-matrix interactions (26). Specifically, **scaffold-free 3D liver spheroid cultures** can be formed from different liver cell sources such as primary human hepatocytes (PHHs), immortalized normal liver cell lines or HCC-derived cell lines (such as HepG2 or HepaRG). Furthermore, growing immortalized or cancer-derived cell lines in liver spheroids promote a more mature hepatic phenotype than the same cells cultured as 2D monolayers, based on hepatocyte functionality and the expression of drug metabolism enzymes and transporters (30).

Multicellular spheroids can be prepared using different approaches such as hanging drop, low attachment plate or magnetic levitation (**Figure 3**). Additionally, **micromolds castings**, which will be utilized for preparing agarose gels followed by spheroid formation. Micromolds for the directed self-assembly of microtissues are flexible, transparent, and could be autoclaved and re-used (31). Different types of micromolds exist, characterised by different sizes, and designed to fit 6-well, up to 96-well tissue culture plates (some examples in **Figure 4A**), sharing some common features (31).

- **A cell-seeding chamber** is a large rectangular recess that collects a single cell suspension and lets cells settle down under gravitational force into the smaller **cell aggregation recesses** (**Figure 4B**).

- **Cell aggregation recesses** locate on the bottom of the agarose gel and extend downward from the floor of the seeding chamber increasing cell-to-cell contact as cells are collected on the concave bottoms of recesses (**Figure 4C; 4D**).

- **Medium exchange ports** help to place a pipet between the gel and the tissue culture plate to change the culture medium and avoid disrupting the cells.

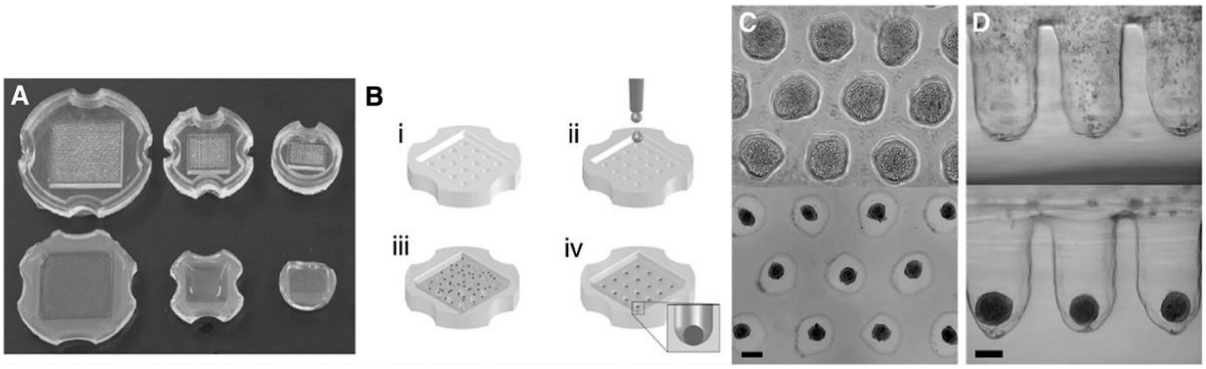

Figure 4. Micromolded nonadhesive gels guide cellular self-assembly. **(A)** Micromolds (top line) used to cast micromolded agarose gels (bottom line) designed to fit different tissue culture plates. **(B)** The self-assembly protocol. Firstly, agarose gels are cast and equilibrated in culture medium (i). Secondly, a cell suspension is added to the seeding chamber, (ii) the cells settle down into the recesses thanks to gravitational force (iii) and interact at the bottom of the concave recesses and self-assemble to form the spheroids (iv). **(C)** Photomicrographs cell suspension (top images) and formed spheroids 24 hours later (bottom images). **(D)** Side-on view of self-assembly of cells in the micromolds. Cells settle into the recesses immediately after seeding (top panels) and form spheroidal microtissues within one day (bottom panels). Scale bars, 200 µm. Adapted from Napolitano AP *et al.* 2007 (31).

When 3D spheroids are designed, an indispensable requirement is cell type selection. Because in the practical part, a liver in vitro cell model was used, we will focus on liver (hepatic) spheroids. The liver comprises hepatocytes, being 70-80% of the cytoplasmic liver mass (32). **PHHs** are widely recognised as the best standard for studying metabolism and liver functions for two main reasons: human origin and expression of relevant human metabolic enzymes (33). On the other hand, their availability is limited, interindividual variation is high, the process of isolation is complex and the behaviour of these hepatocytes in cell culture differs from human body hepatocytes *in situ*, because the lifetime is short, dedifferentiation and loss of hepatocyte functions and phenotypes occur in 2D models rapidly. That is the reason why PHHs are not suitable for routine screening of toxic compounds. **Hepatic carcinoma-derived cell lines** (such as **HepG2 cells)**, and **stem cell-based cultures**, including induced pluripotent stem cells (iPSCs), adult stem cells or embryonic stem cells, are suitable alternatives. These types of cell cultures have almost unlimited growth availability, higher reproducibility of results, and their availability is much higher than in the case of PHHs. Furthermore, these cell lines sustain several phenotypic and functional characteristics of liver cells, mainly in 3D models.

Therefore, they give facilities on cell culturing, and the maintenance of key enzymes involved in metabolism (21).

Currently, progress in automatic image acquisition, analysis, and processing of large amounts of data speed up using of multicellular spheroids as an *in vitro* liver model in drug discovery and toxicology (27). Therefore, a model of multicellular spheroids formed by liver cells was used to study the carcinogenicity potential of chemicals. **The objective of this project was to characterize 3D HepG2 cell CTA assay to establish a new *in vitro* model that adequately mimics *in vivo* model characteristics and will be useful in drug discovery and cancer research, including a potential carcinogenic screening**.

The **specific aims** of the study were:

- To adapt the protocol of a traditional 2D *in vitro* cell transformation assay (CTA) to a 3D CTA assay using scaffold-free spheroids formed by human liver carcinoma HepG2 cells.

- To optimize culture conditions for 3D CTA assay using:

    - **3-methylcholanthrene** (3-MC), a PAH and potent aryl hydrocarbon receptor agonist that is formed as a byproduct of the incomplete combustion of various organic substances like coal, garbage, gas and oil (17,34)**.**

    - **TPA** (phorbol ester 12-O-tetradecanoylphorbol-13- acetate), a hazardous tumor promoter, and an active component of croton oil. TPA is a potent activator of protein kinases C (PKC) and inductor PKC of signalling pathways involved in gene transcription, cell growth, differentiation, programmed cell death, immune pathway, and receptor desensitization (17,35,36).

Materials and Methods

Cell Culture

The HepG2 cells (American Type Culture Collection ATCC®; HB-8065) were cultured in MEM medium (Cat. No. 61100-103; ThermoFisher, Waltham, Massachusetts, USA), containing Earle's salts, L-glutamine and phenol red and further supplemented with 1.5 g/L $NaHCO_3$ (Cat. No. 30067-AP0-G1000-1; LACH-NER, Neratovice, Czech Republic), 1× Non-Essential Amino Acids (Cat. No. M7145; Sigma-Aldrich, Prague, Czech Republic), 1 mM sodium pyruvate (Cat. No. S8636; Sigma-Aldrich) and 10% fetal bovine serum (Cat. No. FB-1001/100; Biosera, Nuaille, France). For the long incubation, the antibiotic normocin (final concentration: 100 mg/mL; Cat. No. ant-nr-1; Invivogen, Huissen, The Netherlands) was added. HepG2 cell line was maintained at 37 °C in a cell incubator at 95% relative humidity and 5% of CO2.

Cells were routinely cultured in the culture medium and Tissue Culture Flask T25 (Cat. No. 92424; TPP, Trasadingen, Switzerland). Cells were sterilely handled (passaging or seeding cells) inside the biosafety cabinet. During the cell passaging, the culture medium was removed from the flask and the cells were washed twice with 2.0-3.0 millilitres (mL) of Phosphate Buffered Saline solution (PBS), containing NaCl 137mM (Cat. No. S3014; Sigma-Aldrich), KCl 2.7 mM (Cat. No. P9541; Sigma-Aldrich), Na2HPO4 8.1 mM (Cat. No. S5136; Sigma-Aldrich), KH2PO4 1.5mM (Cat. No. P5655; Sigma-Aldrich) and deionized water (pH between 7.2-7.4). Then, 500 microlitres (µL) of 1× trypsin-EDTA (Cat. No. XC-T1717; Biosera) were added to the flask and incubated in the incubator for 2-4 minutes (min) to let cells detach from the surface. After checking that cells are adequately detached, 1.5-2.0 mL of MEM medium were added to inhibit the trypsin activity.

Then, the cell clusters (clumps) were resuspended and removed the remaining attached cells by gently pipetting the cell solution several times up and down. Finally, an optic microscope (TCM 400; Labomed, Capelle aan den Ijssel, the Netherlands) was used to check if HepG2 cells were properly separated. If necessary, a needle was used to separate cells properly to get a single-cell solution. At this point, a part of the cell suspension was transferred to a new flask; 20 µL of cell suspension were pipetted in a slide to calculate cell concentration using an automated cell counter (Nexcelom Bioscience, Lawrence, MA, USA), and finally the rest of the cell suspension was used for cell seeding to form 3D spheroids.

Three-Dimensional Cell Culture

- 3D Petri Dish® Casting

The 3D HepG2 cell spheroids were created using 3D Petri Dish® cast with 35 recesses. In brief, the molten agarose was first prepared, specifically 2% agarose (w/v; Cat. No. A9539-10G; Sigma-Aldrich) solution dissolving 1 gram (g) of agarose in 50 mL of 0.9% NaCl (Cat. No. 7647-14-15; mikroCHEM, Pezinok, Eslovakia) and autoclave it. The micro-molds for casting 3D Petri Dishes® were also autoclaved before use. On an experimental day, agarose solution was boiled in the microwave to dissolve the agarose powder completely. Then, the molten agarose was placed in a 50 mL centrifuge tube in a thermoblock set up at 70ºC inside the laminar hood to maintain the aseptic conditions.

Next, in a biosafety cabinet using the aseptic technique, 330 µL of molten agarose were pipetted into a 24-series micromold. After the agarose has gelled, the micromold was carefully flexed to remove the 3D Petri Dish®. Then, each 3D Petri Dish® (a micromolded agarose gel) was transferred to a well in a 24-well tissue culture plate (TTP) and organised aligned in the same position. Finally, to immobilize micromolded gels,130 µL of molten agarose (45˚C) were pipetted into each well around each micromolded gel.

- Equilibration

To equilibrate 3D Petri Dish®, 1.0 mL of the culture medium was added to each well containing the agarose gel and incubated it overnight in an incubator.

- Cell Seeding the 3D Petri Dish®

The next day, cell splitting and seeding into each micromolded gel were carried out. The cell specification (the number of passages in monolayer cell culture, the number of cells per spheroids and per plate, and the volume needed) is in **Table 1**. The cell culture MEM medium was carefully removed from the outside of the 3D Petri Dish® and its inner chamber, trying not to damage the agarose gel. The cell suspension (65 µl with 4,000 cells per spheroids, i.e. 140,000 cells in total per each 3D Petri Dish®) was added, dropwise, into the cell seeding chamber.

Table 1. Resume information about cell concentration and volume needed for cell seeding calculations.

Nº Plate	Plate A	Plate B	Plate C
2D HepG2 Cell passage	p13/p9	p13/p9	p2/p15
Cells per spheroid	4.000 cells per spheroids	4.000 cells per spheroids	4.000 cells per spheroids
Cells needed for all spheroids per plate	3, 36 × 106	3, 36 × 106	3, 36 × 106
Volume per well	65 µl	65 µl	65 µl
Final Volume per plate	1560 µl	1560 µl	1560 µl

After the seeding into the 3D Petri Dish® agarose gel, the cells were allowed (~10 min) to settle into the features (recesses) of the 3D Petri Dish®. Finally, 1.0 mL of the additional MEM medium was added to the outside of the agarose gel. Then, 24 well-plate was placed into the incubator and the culture medium was exchanged as needed.

3D HepG2 Cell-based Transformation Assay

Figure 5 shows a schema of the 3D HepG2 cell-based transformation assay. The spheroids were exposed as compact mature spheroids on the fourth day in the culture. The culture or exposure (the culture medium with the solvent or chemical) media were changed on the 4^{th}, 7^{th}, 8^{th}, 10^{th}, 14^{th}, 17^{th}, 21^{st} and 24^{th} day.

It is important to emphasize that there were five different exposure (treatment) conditions within a 28-day protocol:

- **Untreated spheroids (negative control, NC).** The spheroids were incubated with the culture medium for the whole incubation/exposure time (28 days). The NC was in tetraplicate (35 spheroids per well × 4 wells = 140 spheroids).

- **Solvent treated control spheroids (solvent control, SC).** The spheroids were treated with dimethyl sulfoxide (DMSO, Cat. No. C6614; Sigma-Aldrich) at the final concentration of 1.55× (v/v) on the 4th day, then with ethanol (EtOH; Cat. No. 493511; Sigma-Aldrich) at the final concentration of 1.0× % (v/v) on the 7th, 8th, 10th, 14th, 17th, 21st and 24th day. The SC was in tetraplicate (35 spheroids per well × 4 wells = 140 spheroids).

- **3-MC alone treated spheroids (3-MC).** The spheroids were exposed to 3-MC (98% purity, Cat. No. 213942; Sigma-Aldrich) at the final concentration of 2 mg/mL on the 4th day and the rest of the days just with the culture medium. The 3-MC variant was in tetraplicate (35 spheroids per well × 4 wells = 140 spheroids).

- **TPA alone treated spheroids (TPA)**. The spheroids were incubated with just the culture medium for the first six days, then exposed to TPA (≥98% purity, Cat. No. 16561-29-8; Sigma-Aldrich) on the 7th, 8th, 10th, 14th, 17th, 21st, and 24th day. The TPA variant was in tetraplicate (35 spheroids per well × 4 wells = 140 spheroids).

- **3-MC and TPA treated spheroids (3-MC + TPA).** The spheroids were exposed to 3-MC at the final concentration of 2 □g/mL on the 4th day, then exposed to TPA at the final concentration of 0.1 □g/mL on the 7th, 8th, 10th, 14th, 17th, 21st, and 24th.The 3-MC+TPA variant was in eight plicate (35 spheroids per well × 8 wells = 280 spheroids).

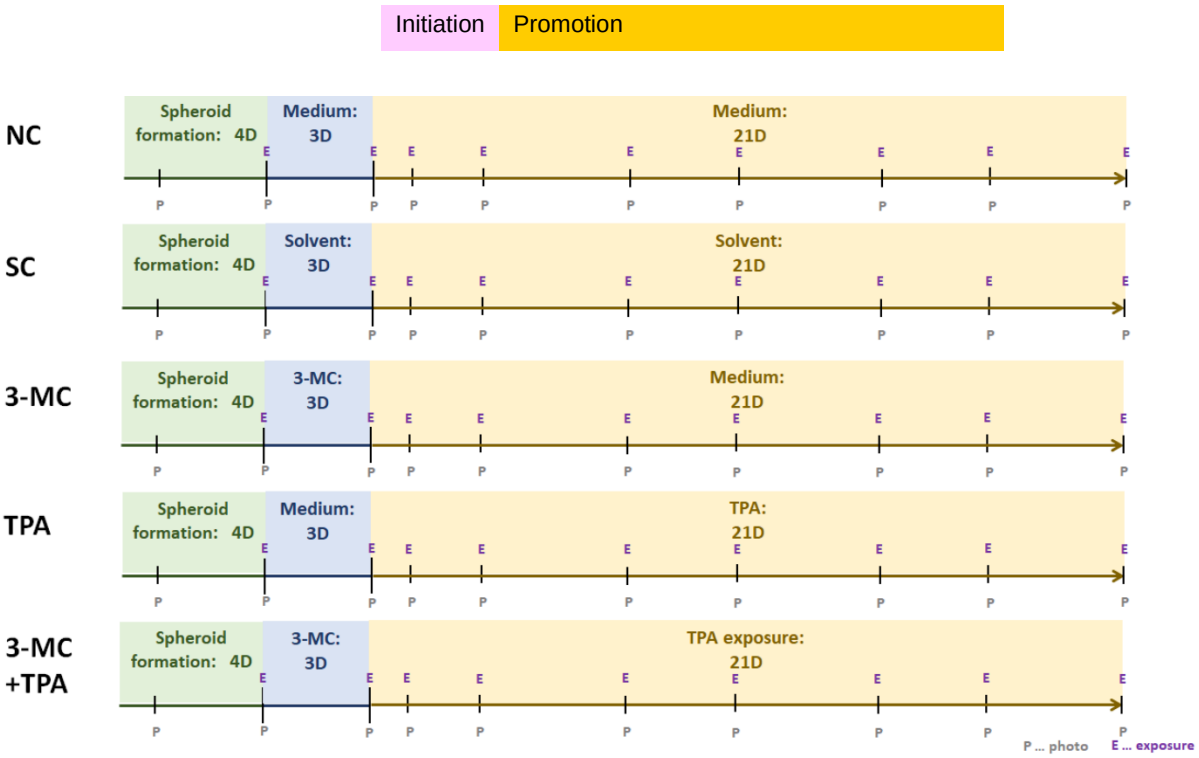

Figure 5. The schema of 3D HepG2 cell-based transformation assay. NC: negative control; SC: solvent control. 4D: four days interval; 3D: three days interval where 3-MC exposure occurs, starting the initiation phase of carcinogenic process; 21D: twenty one days interval where TPA exposure occurs, starting the promotion phase. Each vertical bar represents days 1, 4, 7, 8, 10, 14, 17, 21, 24 and 28 from left to right. Chemical exposure was stopped on day 24.

Image Acquisition

Brightfield spheroid images were taken on the 1st, 4th, 7th, 8th, 10th, 14th, 17th, 21st, and 24th day. Images were acquired using the automated imaging system TissueFAXS equipped with a CMOS Baumer XG40c, using 2.5× objective as reported previously (16). The spheroids in the first well were manually focussed. Then, different parameters were adjusted, such as saturation, gamma, exposure time, white balance. The focus was either confirmed or re-adjusted by the user for the subsequent wells throughout the acquisition. After that, the entire microplate was scanned in the preview mode first, then the region of interest (ROS) covering the whole spheroid array was defined for each hydrogel/microplate well and saved. Thanks to the adhesion of the agarose gels to the surface of the plate in a specific position, the template

with defined regions can be saved and used for repeated image acquisitions from the same plate. Once the photos were acquired, they were saved, stitched and exported with a region overview and a 100% increased.

Image Analysis

Image analysis was carried out using Fiji, an image processing package based on ImageJ (37,38). The Fiji/ImageJ programming language Jython was used to create a macro called the 'Spheroid.Macro.ijm', which is designed to automatically detect spheroids in microphotographs in .jpg, .tiff and or .png format (16). It allows the evaluation of multiple spheroids per single image, including composite images of multiple fields of view.

Firstly, in Analyze option in the toolbar, the following measurements were set: area, minimum and maximum gray values, center of mass, bounding rectangle, shape descriptors, integrate density, skewness, area fraction, centroid, perimeter, flit ellipse, Feret´s diameter, median. Nextly, in Plugin's option, installed the ´Spheroid.Macro.ijm ´ and opened all the images through the SpheroidMacro. The scale was set up at 2.143 mm/pixel, size between 18000-infinity and circularity was change depending on the image, being a number closer to zero less circular, and closer to one more circular. After that, the output result file showed the expected number of spheroids per image, and for each spheroid identified, the macro provided two main types of measurements:

- **Size measurements** (Table 2) represented**:** area (µm2), the diameter of the fitted ellipse (major and minor axis, µm), Feret's maximum and minimum diameter (µm), Feret´s diameter (µm), perimeter (µm) and volume.

- **Shape** (Table 3) **measurements** represented: circularity (sphericity), aspect ratio, roundness, and solidity.

- All the measurements obtained from each picture will be sump up in an excel file for further analysis.

Table 2. Measured size parameters of spheroids (39,40,41).

Size Parameters			
	Unit	**Characteristics**	**Formula**
Feret´s Diameter	mm	The longest distance between any two points along the selection boundary	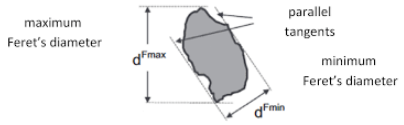
Volume	mm^3	The amount of space occupied by a three-dimensional object	$Vol = \frac{1}{6} \times \pi \times [Major\ axis]^2 \times [Minor\ axis]$
Perimeter	mm	The length of the outside boundary of the selection	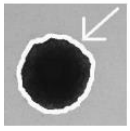
Area	mm^2	Expresses the extent of a 2D region, shape, or planar lamina, in the plan. Calculated in ImageJ as the sum of the areas of each individual pixel, a_p.	$A = \sum a_p$

Table 3. Measured shape parameters of spheroids (39,40).

Shape Parameters			
	Unit	**Characteristics**	**Formula**
Solidity	Dimensionless	Measurement of the overall concavity of a particle	$Solid = \frac{[Area]}{[Convex\ area]}$
Roundness	Dimensionless	Specifies the deviation from the circular shape. As particle becomes circular, value approaches one.	$Round = \frac{4 \times [Area]}{\pi \times [\text{Major } Axis]^2}$
Circularity	Dimensionless	Specifies ideally circular object. A value of 1.0 indicating a perfect circle. As the value approaches 0.0, it indicates an increasingly elongated shape.	$Circ = \sqrt{\frac{4 \times \pi \times [Area]}{[Perim]^2}}$
Aspect Ratio (AR)	Dimensionless	Maximum horizontal and vertical distances.	$AR = \frac{[Major\ axis]}{[Minor\ axis]}$

Spheroid’s Harvesting

To harvest spheroids, a new 24 wells plate was filled with PBS: 500mL per well. The gels with spheroids were transferred to this new plate with PBS solution. The gels were turned upside down and centrifuged for 3 min at 200 × g (5810 R Eppendorf, Říčany u Prahy, Czech Republic). Next, the spheroids for each variant (NC, SC, 3-MC, TPA, 3-MC+TPA) in PBS were transfer from a well to an Eppendorf. Eppendorf tubes were centrifuged, the supernatant was discarded, and spheroids were washed one more time with PBS. Finally, 500 mL of trizol (Cat. No. 15596018; Invitrogen, Waltham, MA, USA) were added, and the samples were stored in a freezer at -80C. Later on, RNA was isolated from these samples and reverse transcripted to cDNA. Then, the expression of genes associates with neoplastic and hepatocellular carcinoma cell lines phenotypes will be evaluated using RT-qPCR.

Statistical Analysis

Data expressed represented three independent experiments and presented as an average of these three experiments with standard deviation. Data related to the parameters with dimension (area, volume, perimeter, Feret´s diameter) were normalized to untreated controls for each exposure time and expressed as a percentage of untreated spheroids. Graphs were plotted using **Graphpad Prism 4** (Graphpad software). Statistical analysis was carried out using **one-way ANOVA** with Dunnett´s post hoc test or **two-tailed Student´s t-test** after confirming data normality and equal variance.

Results

Spheroid Formation and Structure

Spheroids of liver HepG2 cells were prepared using the 3D Petri Dish® micro-mold casting. The seeding density was 4,000 cells per spheroid. The spheroid formation and maturation were monitored by microscopic evaluation on the day 1, 4, 7, 8, 10, 14, 17, 21, 24 and 28 of spheroid culture. The parameters describing the spheroid size (area, volume, perimeter, Feret's diameter) and shape (circularity, roundness, aspect ratio, solidity) were analysed. The representative images of non-treated HepG2 spheroids are shown in **Figure 6.** After the first 24 hours, spheroids have already been formed, with the area around 155,132 mm^2, the volume around 2.98×10^7 mm^3, the perimeter 1339 mm, and the Feret's diameter around 434 mm (F**igure 7**). Their shape was irregular with low circularity (around 0.74) and roundness (around 0.917) and high AR (around 1.09) (**Figure 8**).

The 1-day spheroids were not compact with solidity around 0.96. However, during the next three days (Day 1 to Day 4), the size of spheroids (area, perimeter and Feret's diameter) significantly decreased (**Figure 7**: area: *p≤0.05; perimeter: **p ≤ 0.01; and Feret's diameter: ***p ≤ 0.001; one-way ANOVA with Dunnett's post hoc test), reaching the minimum value for these parameters among all the days. Additionally, their shape and compactness improved with circularity and solidity significantly higher (**Figure 8**: **p ≤ 0.01; ***p ≤ 0.001; one-way ANOVA with Dunnett's post hoc test). Thus, the compact, circular and round spheroids were formed on day 4. Between days 4 and 28, the HepG2 spheroids slowly grew and kept their circularity, roundness, AR and solidity at a similar level (**Figure 8**).

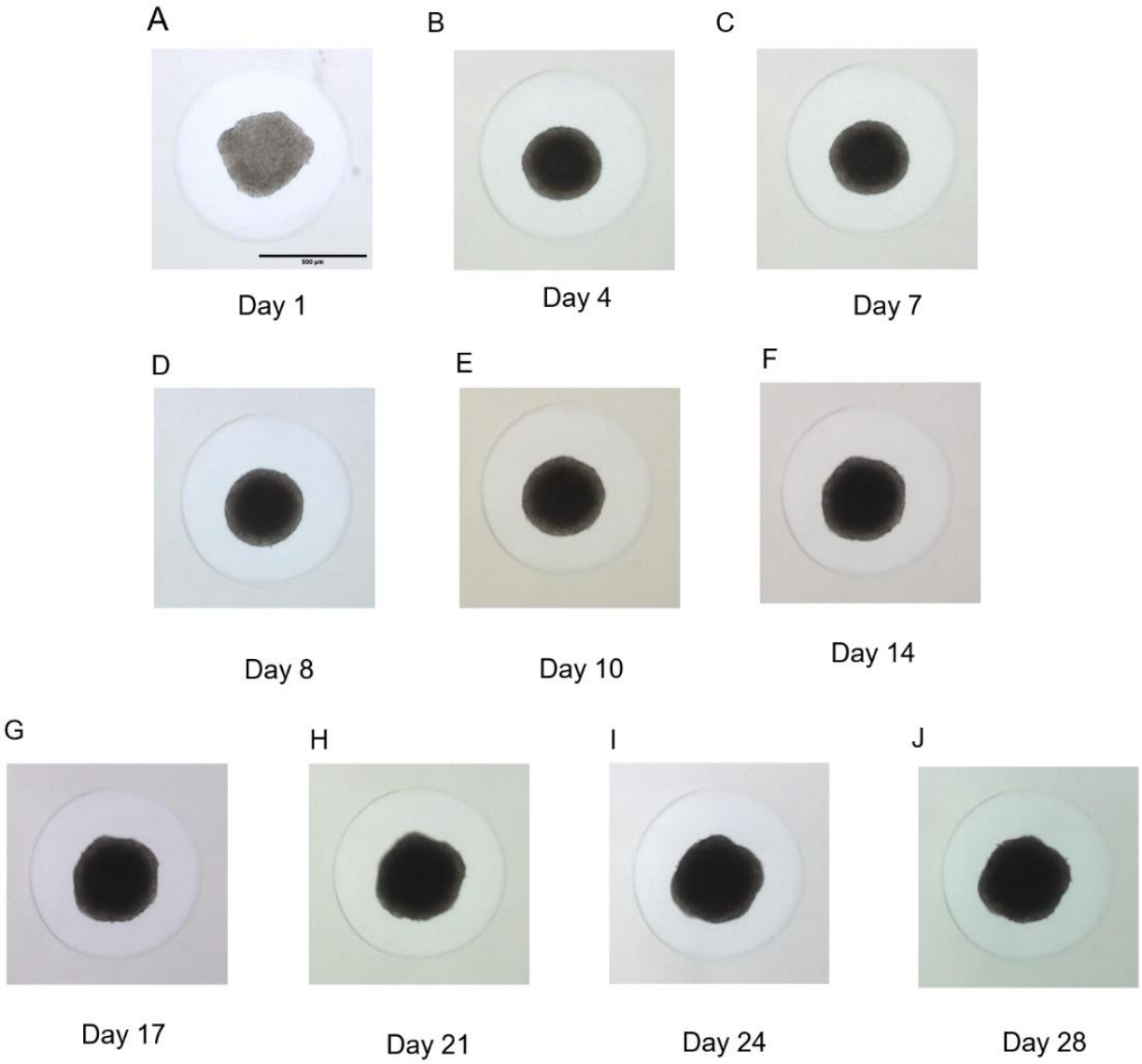

Figure 6. The representative images of 3D HepG2 spheroids monitored by automatic microscopic platform TissueFAXS showing their formation and maturation within the culture. HepG2 cells were seeded into 2% agarose gels at a density of 4000 cells per spheroid. Scale bars represent 500 µm.

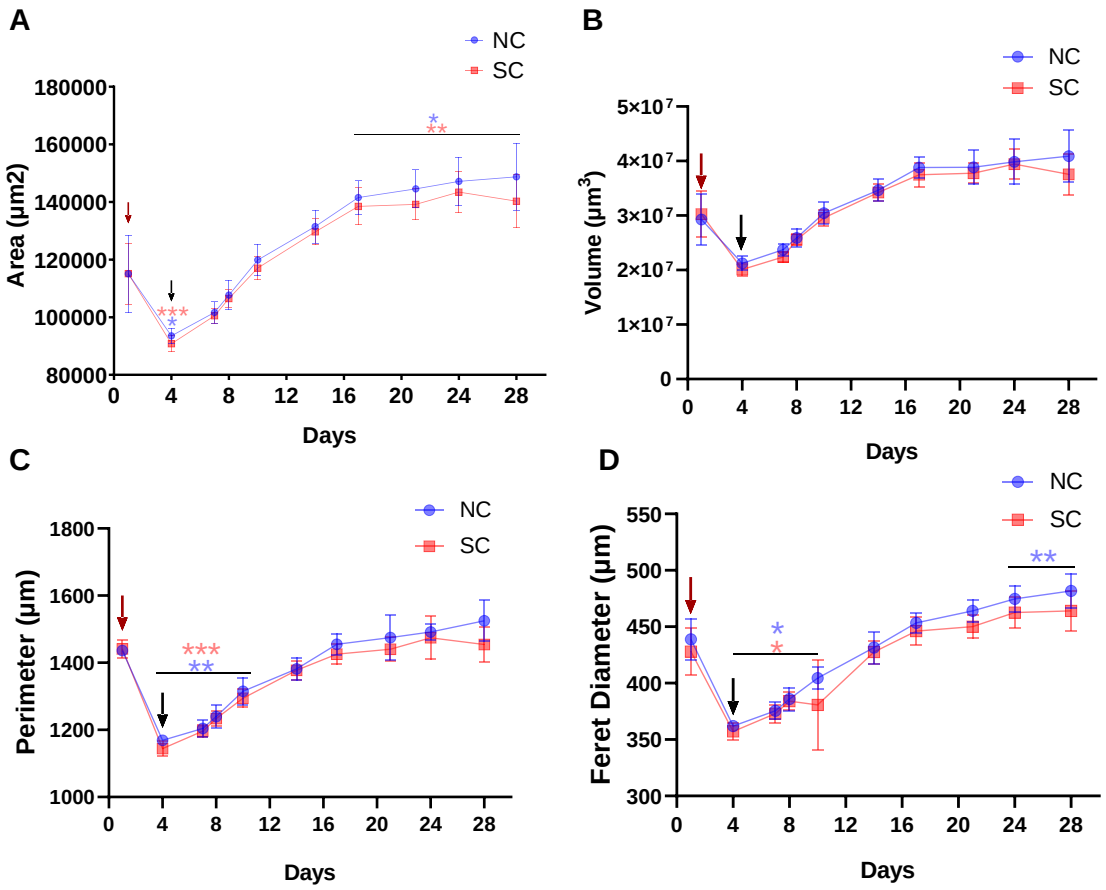

Figure 7. The size of the untreated spheroids (NC) and the spheroids treated with solvent (SC) within time. Each size parameter (A. area, B. volume, C. perimeter and D. Feret's diameter) is expressed as average from three independent experiments with standard deviation (n=3). The asterisk represents statistical significance from the spheroids on day 1 (*P≤0.05, **P ≤ 0.01, ***P ≤ 0.001; one-way ANOVA with Dunnett's post hoc test). There was no statistical difference between parameter values for NS and SC for any exposure time ($p > 0.05$, two-tailed Student´s t-test). The red arrow in the graphs indicates the size of 1-day spheroids (24 hours after cell seeding), the black arrow indicates when the chemical exposure started (4 days after cell seeding).

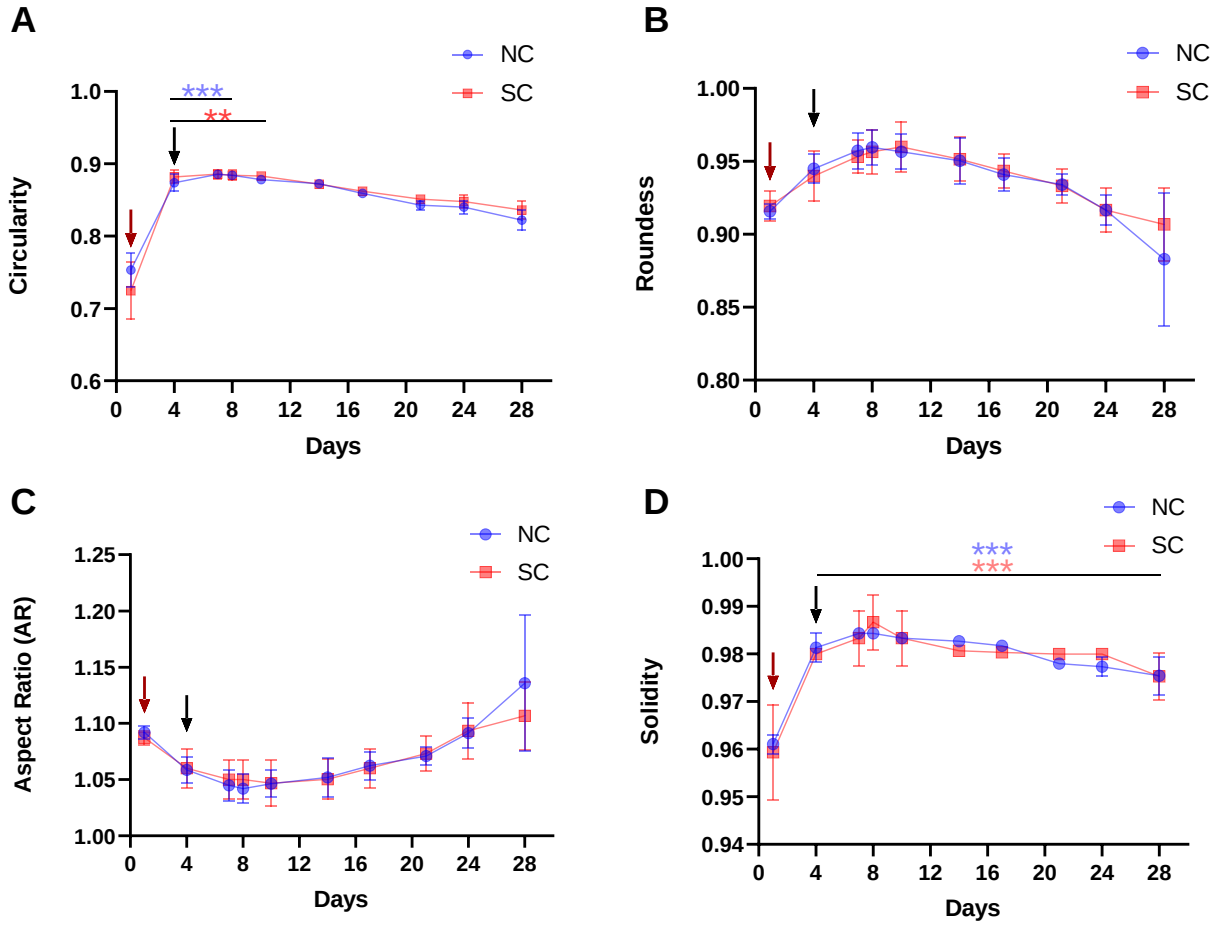

Figure 8. The shape of untreated spheroids (NC) and the spheroids treated with solvent (SC) within time. Each shape parameter (A. circularity, B. roundness, C. aspect ratio, D. solidity) is expressed as average from three independent experiments with standard deviation (n=3). The asterisk represents statistical significance from the spheroids on day 1 (*P≤0.05, **P ≤ 0.01, ***P ≤ 0.001; one-way ANOVA with Dunnett's post hoc test). There was no statistical difference between parameter values for NS and SC for any exposure time ($p > 0.05$, two-tailed Student´s t-test). The red arrow in the graphs indicates the size of 1-day spheroids (24 hours after cell seeding), the black arrow indicates when the chemical exposure started (4 days after cell seeding).

3D HepG2 transformation assay

The spheroids were exposed on day 4 when the spheroids were already compact and regular (**Figure 6-8**) after self-assembling and self-compacting. The exposure schema is in Figure 5. Firstly, it was essential to demonstrate that DMSO and EtOH used as solvent control do not affect spheroid size or shape. Therefore, we compared the SC with untreated control NC for each parameter and exposure time (**Figure 7 and 8**), and no statistical significance was confirmed (two-tailed Student´s t-test). Thus, the solvent-treated spheroids mimicked the behaviour of non-treated spheroids within the culture concerning their size and shape (**Figure 9 and 10**). The HepG2 spheroids were exposed to 3-MC alone (2 mg-mL) for the first three days (Day 4-Day 7), TPA alone for 21 days (Day 7-Day 28) and 3-MC+TPA, where the spheroids were exposed to 3-MC (Day 4-Day 7) followed by TPA exposure for 21 days (Day 7-Day 28). The morphology of spheroids treated with solvent, 3-MC alone, TPA alone and 3-MC+TPA is shown in **Figure 9** for the illustration.

3-MC alone significantly reduced the spheroid size (**Figure 10**) and disturbed their shape and compactness (**Figure 11**). All parameters representing size gradually decreased within time, reaching their minimum around day 14, with the area around 54% of non-trated spheroids, volume 40%, perimeter 77%, and Feret's diameter around 108% (perimeter, Feret's diameter **p ≤ 0.01; area, volume: ***p ≤ 0.01; two-tailed t-test). Their shape was irregular with low circularity (minimum around 0.73%; circularity, *p ≤ 0.05) and solidity (minimum around 0.94%; ***p ≤ 0.01) than for solvent control on the last days (Day 14 to 28) (**Figure 11**) compared to SC spheroids. Both parameters were decreasing within the entire exposure. As a result, the border of spheroids became irregular and less compact, and cell debris appeared around spheroids (**Figure 9**).

TPA alone significantly increased spheroid perimeter (**Figure 10**) and reduced circularity and solidity (**Figure 11**). The perimeter is significantly bigger from day 8 until the end of the exposure (maximum 108%; *p ≤ 0.05; two-tailed t-test). Futhermore, TPA caused the irregular shape of spheroids with lower circularity (minimum around 0.73%; **p ≤ 0.01; two-tailed t-test) and solidity (minimum around 0.95%; *p ≤ 0.05; two-tailed t-test) than solvent control (**Figure 11**).

The size and shape of **3-MC + TPA-treated spheroids** were similar to 3-MC treated spheroids.They were significantly reduced in the spheroid size (**Figure 10**) and shape (**Figure 11**). All parameters representing size (area, volume, perimeter, Feret's diameter) and circularity and solidity parameters, gradually decreased within time. Size measures reached their minimum around day 14 (perimeter: *p ≤ 0.05; Feret's diameter **p ≤ 0.01; area, volume: ***p ≤ 0.05) and keeping it by the end of the exposure, in contrast to circularity and solidity their minimun was reached around day 24. In addition, as 3-MC alone, 3-MC+TPA caused the irregular shape of spheroids with lower circularity and solidity (compactness) than SC. Both parameters were decreasing within the entire exposure (circularity minimum around 0,72, *p ≤ 0.05; solidity minimun 0,944 ***p ≤ 0.01; two-tailed t-test). As a result, the border of spheroids became irregular and less compact, and cell debris appeared around spheroids (**Figure 9**).

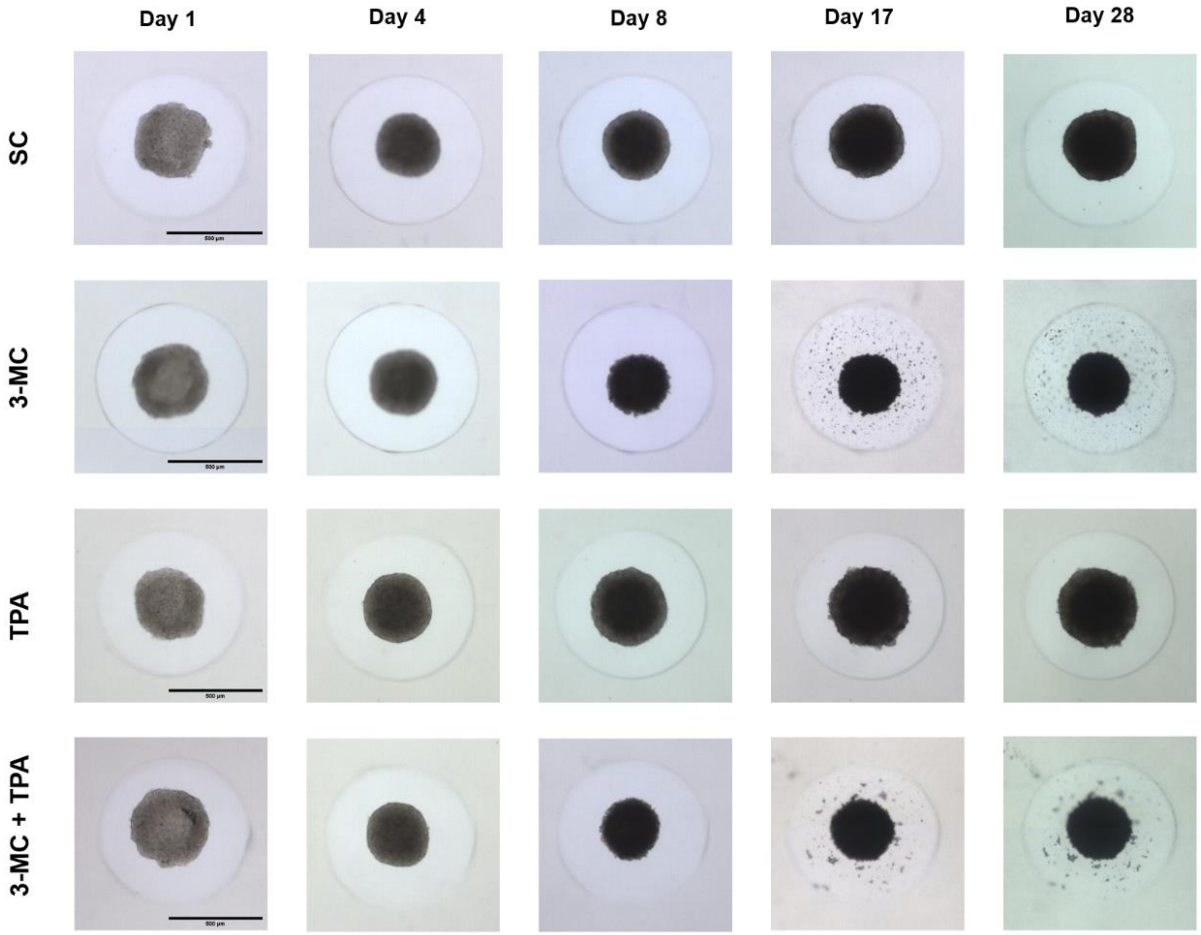

Figure 9. Effect of 3-MC alone, TPA alone and 3-MC+TPA treatment on HepG2 spheroid morphology. The representative images are shown. The spheroid morphology was monitored by the automatic microscopic platform TissueFAXS. HepG2 cells were seeded into 2% agarose gels at a density of 4000 cells per spheroid. Scale bars represent 500 µm.

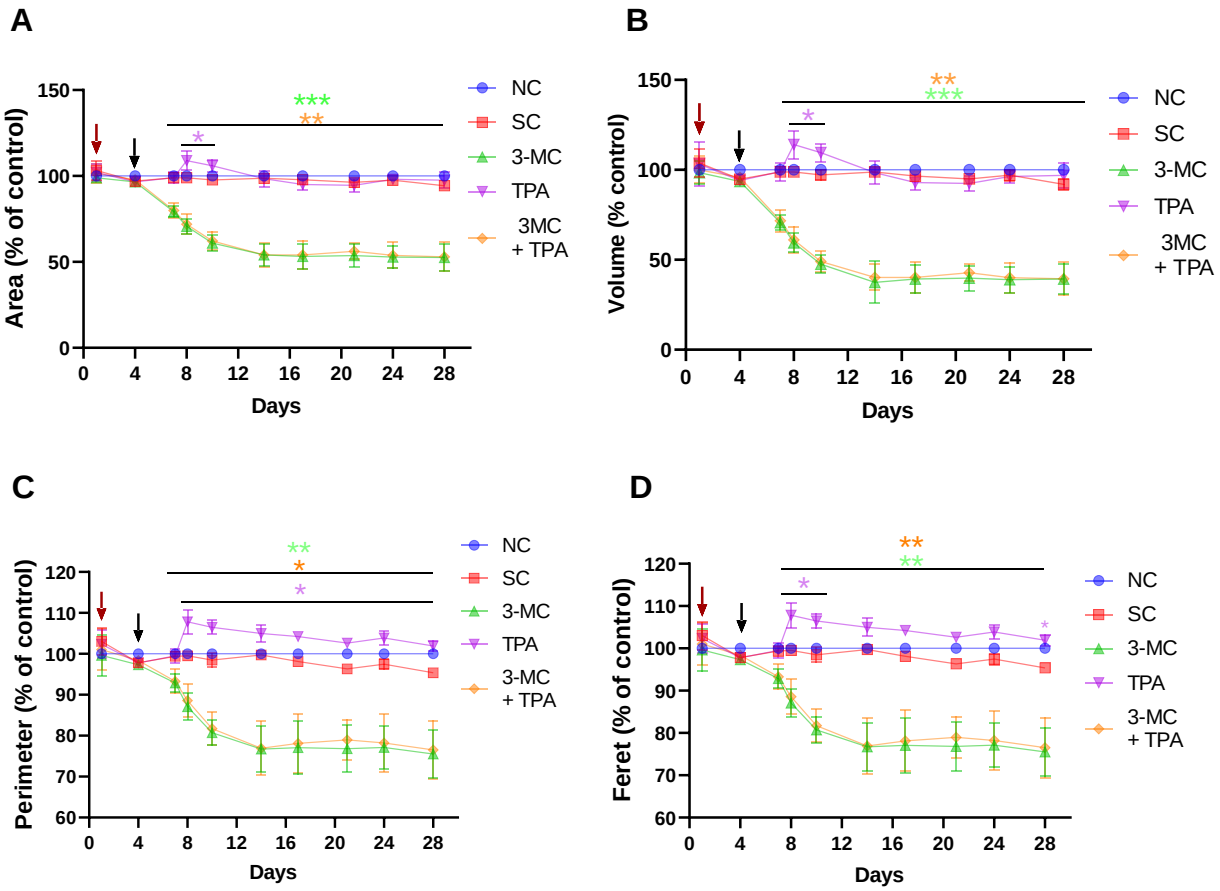

Figure 10. Effect of 3-MC alone, TPA alone and 3-MC+TPA treatment on HepG2 spheroid size. Each parameter (A. area, B. volume, C. perimeter and D. Feret's diameter) is expressed as average from three independent experiments with standard deviation (n=3) represented by the average values obtained from three independent experiments (n=3). The asterisk represents statistical significance from a corresponding solvent control (*P≤0.05, **P≤0.01, ***P≤0.001; two-tailed t-test). The red arrow in the graphs indicates the size of 1-day spheroids (24 hours after cell seeding), the black arrow indicates when the chemical exposure started (4 days after cell seeding). NC, non-treated spheroids (negative control); SC, solvent-treated spheroids (solvent control).

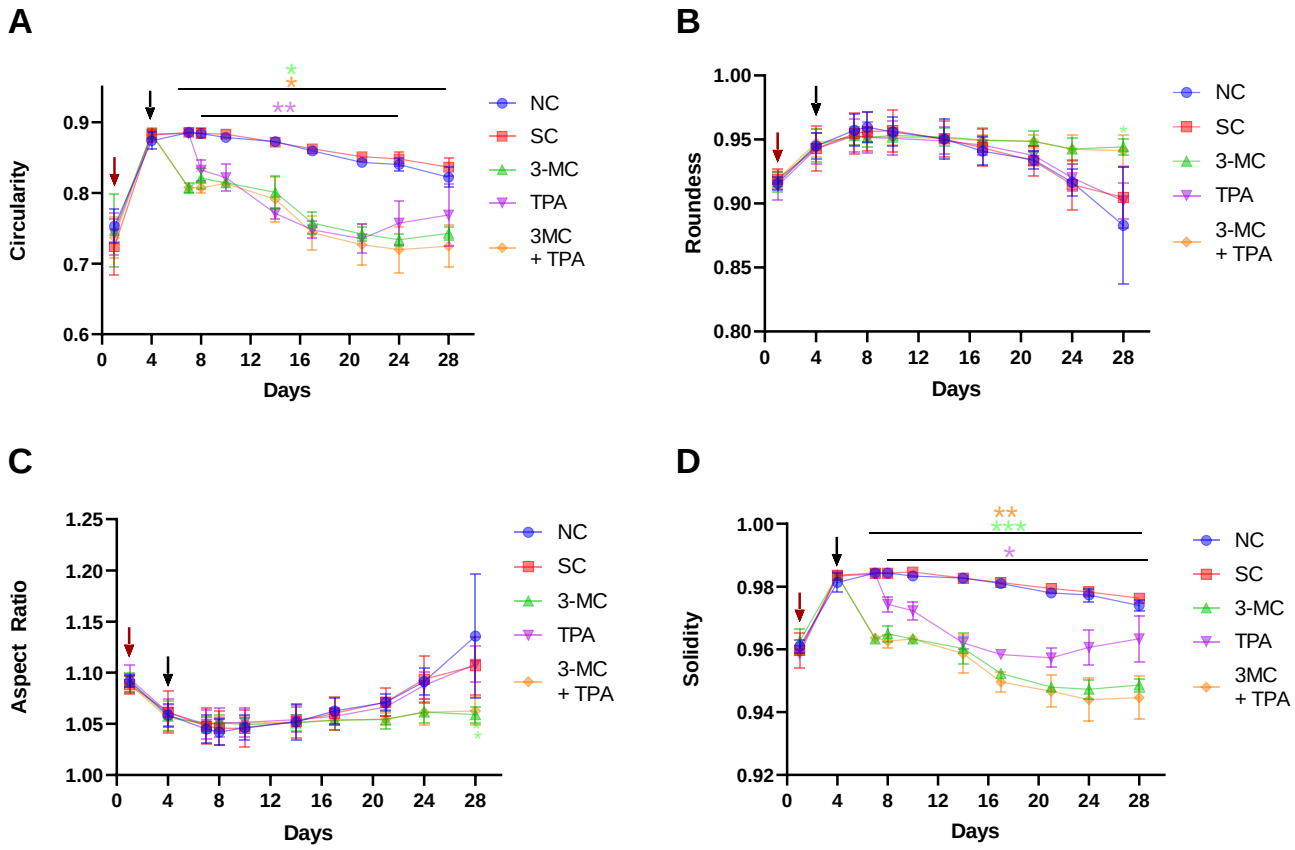

Figure 11. Effect of 3-MC alone, TPA alone and 3-MC+TPA treatment on HepG2 spheroid shape. Each parameter (A. area, B. volume, C. perimeter and D. Feret's diameter) is expressed as average from three independent experiments with standard deviation (n=3). The asterisk represents statistical significance from a corresponding solvent control (*P≤0.05, **P≤0.01, ***P≤0.001; two-tailed t-test). The red arrow in the graphs indicates the size of 1-day spheroids (24 hours after cell seeding), the black arrow indicates when the chemical exposure started (4 days after cell seeding). NC, non-treated spheroids (negative control); SC, solvent-treated spheroids (solvent control).

Discussion and Conclusions

3D cell culture models are an attractive alternative to the 2D cell culture *in vitro* model. Thus, continuous development in the 3D mammalian cell culture systems improves cell-cell and cell-ECM interactions and specific functionality, availability, reproducibility, scalability, and affordability (9,12). Among the 3D cell models, scaffold-free 3D spheroid cultures represent a suitable in vitro model for screening purposes, and it is increasingly used as a new 3D culture technique. The spheroids mimic a close physiological microenvironment characteristic of physiological tissues or tumors, maintaining normal cell characteristics related to cell-cell, and cell-ECM contacts (12).

Carcinogenesis is recognized as a multipath process in which distinct molecular and cellular alterations occur, consisting of separate but closely linked stages of **initiation**, where mutations or gene alteration arise **promotion**, where preneoplastic cells proliferate and accumulate, and **progression**, the final stage of neoplastic transformation (5,10). Therefore, different transformation assays could be performed with exogenous initiating (3-MC, DMBA) and promoting (TPA) chemical carcinogens to induce carcinogenesis process.

Traditionally, animals are required to assess the carcinogenic potential of chemicals despite their ethical, practical, and economic limitations (13). In addition, with the implementation of the 3R principles, new efficient *in vitro* cell models are in continuous development and should refine animal-based testing even for carcinogenicity assessment and research. Traditional 2D CTAs use **2D models** of different cell lines, namely SHE, BALB/c 3T or Bhas 42 cells (14,19,42). The **2D** models generally are characterized by the growth of the cells in a flat monolayer, attached to the stiff surface. The main disadvantage of 2D models is the lack of biological functions due to limited cell-to-cell and cell-to matrix interactions, resulting in loss of cell differentiation, modification in signalling pathways and depletion of the expression of important enzymes, which can consequence in misleading results (16,20). That is maybe why these CTAs, even after their validation, were not considered alternatives for assessing chemicals' carcinogenic potential yet (14)

Newly alternative developed 3D cell culture models, including 3D liver models, present a better cell-cell interaction and similarity to *in vivo* situation. Specifically, 3D liver models have a higher levels of liver-specific functions, including metabolic enzyme activities as well as cell morphology and biochemical properties, which reflect in vivo conditions in the liver more

accurately (20). That is why it is important to establish a new hepatic in vitro model that mimics as much as possible the liver microenvironment, including the tumor carcinogenic cell environment.

From our results, it is clear that**,** for a seeding density of 4000 HepG2 cells per spheroids 4 days are necessary to self-assembly and self- compactness. The spheroids self-assembly and self-compactness affect to their area, perimeter, Feret's diameter, circularity and solidity during the first four days. On the other hand, the volume of the spheroids did not significantly change within time, suggesting that the spheroid volume do not change during the time of spheroids culture. The roundness and AR of spheroids also did not significantly change within time, suggesting that the roundness and AR of spheroids do not change during the time of spheroids culture. From day 4, steady growth of spheroids during the time of culture appeared without shape changes. The protocol for HepG2 spheroids has been optimized and was reproducible independently.

In addition, we developed and optimized a new 3D HepG2 cell-based transformation assay. We adopted the protocols of 2D CTAs, where 3-MC was successfully applied as an initiator and TPA as a tumor promotor. We used their effective concentrations and exposure times for these 2D models. We monitored spheroid size and shape within the entire exposure. After self-assembly, the compact and mature spheroids were exposed. The spheroids treated with DMSO or ethanol as solvent control did not differ from the non-treated spheroids in area, volume, perimeter Feret's diameter size and shape parameters. The spheroids treated with **3-MC and TPA** or **3-MC** alone were characterized by smaller size and irregular shape, especially low circularity and irregular spheroid border, and lower compactness (solidity). In contrast, roundness and AR values were not significantly altered. Similarly, the spheroids treated with **TPA alone** had similar roundness and AR as the control ones. On the other hand, their perimeter, area, volume and Feret's diameter were higher and circularity and solidity lower. The changes induced by 3-MC, TPA and 3-MC+TPA suggest that these exposure variants can lead to alternations related to their carcinogenicity potential (13,19).

However, to confirm cell transformation in the exposed spheroids, it is necessary to evaluate the expression of genes associates with neoplastic and hepatocellular carcinoma cell lines phenotypes using RT-qPCR. Therefore, we will focus on the genes involved in 1) the regulation of cell proliferation, regeneration and apoptosis (PCNA, Cyclin D1, p-S6, Ki67, Bcl-2); 2) drug resistance (MDR1, MRP2, BCRP) and 3) adhesion and epithelium mesenchymal transition

(MMP-2/9 or E-cadherin/N-cadherin) (43). In parallel, the functionality of spheroids will be assessed by measuring albumin, urea or lactate in the collected medium (18,43).

In **conclusion**, the 3D CTA assay utilizing 3D spheroid models of HepG2 cells can be a promising tool for screening carcinogenicity potential of chemicals or new anti-cancer in biomedical, pharmacological and toxicological research and their applications. However, this assay needs further optimization and validation to confirm its potential.

References

1. World Health Organization; Health Topic; Cancer. 04-03-2021. Available from: https://www.who.int/health-topics/cancer#tab=tab_1

2. Shaw E, Farris MS, Stone CR, Derksen JWG, Johnson R, Hilsden RJ, *et al.* Effects of Physical Activity on Colorectal Cancer Risk Among Family History and Body Mass Index Subgroups: A Systematic Review and Meta-Analysis. BMC Cancer. 2018; 18: 71. doi: 10.1186/s12885-017-3970-5.

3. Madia F, Worth A, Whelam M, Corvi R. Carcinogenicity Assessment Addressing the Challenges of Cancer and Chemicals in the Environment. Environ Int. 2019; 128: 417–29. doi: 10.1016/j.envint.2019.04.067.

4. Lewandowska A, Rudzki M, Rudzki S, Lewandowski T, Laskowska B. Environmental Risk Factors for Cancer – Review Paper. Ann Agric Environ Med. 2019; 26: 1–7. doi: 10.26444/aaem/94299.

5. Jacobs MN, Colacci A, Corvi R, Vaccari M, Aguila MC, Corvaro M, *et al*. Chemical Carcinogen Safety Testing: OECD Expert Group International Consensus on the Development of an Integrated Approach for the Testing and Assessment of Chemical Non-Genotoxic Carcinogens. Arch Toxicol. 2020; 94: 2899–923. doi: 10.1007/s00204-020-02784-5.

6. World Health Organization; International Programme on Chemical Safety. 04-03-2021. Available from: https://www.who.int/health-topics/chemical-safety#tab=tab_1

7. NIH, National Cancer Institute. 08-03-2021. Available from: https://www.cancer.gov/publications/dictionaries/cancer-terms/def/carcinogenesis

8. Bevan RJ. Threshold and Non-threshold Chemical Carcinogens: A Survey of the Present Regulatory Landscape. Regul Toxicol Pharmacol. 2017; 88: 291-302. doi: 10.1016/j.yrtph.2017.01.003.

9. Cornel C, Alecsandru Ioan B. Comparative Oncology. The Publishing House of the Romanian Academy; 2007. Available from: https://www.ncbi.nlm.nih.gov/books/NBK9552/

10. Greten FR, Grivennikov SI. Inflammation and Cancer: Triggers, Mechanisms, and Consequences. Immunity. 2019; 51: 27–41. doi: 10.1016/j.immuni.2019.06.025.

11. Siddiqui IA, Sanna V, Ahmad N, Sechi M, Mukhtar H. Resveratrol Nanoformulation for Cancer Prevention and Therapy: Resveratrol Nanoformulations for Cancer. Ann N Y Acad Sci. 2015; 1348: 20–31. doi: 10.1111/nyas.12811.

12. Basu A. DNA Damage, Mutagenesis and Cancer. Int J Mol Sci. 2018; 19: 970. doi: 10.3390/ijms19040970.

13. Cohen SM, Boobis AR, Dellarco VL, Doe JE, Fenner-Crisp PA, Moretto A, *et al*. Chemical Carcinogenicity Revisited 3: Risk Assessment of Carcinogenic Potential Based on the Current State of Knowledge of Carcinogenesis in Humans. Regul Toxicol Pharmacol. 2019; 103: 100–5. doi: 10.1016/j.yrtph.2019.01.017.

14. Mascolo MG, Perdichizzi S, Vaccari M, Rotondo F, Zanzi C, Grilli S, *et al*. The Transformics Assay: First Steps for the Development of an Integrated Approach to Investigate the Malignant Cell Transformation in Vitro. Carcinogenesis. 2018; 39: 955–67. doi: 10.1093/carcin/bgy037.

15. Toxicity Testing in the 21st Century: A Vision and a Strategy. Washington, D.C.: National Academies Press; 2007. Available from: http://www.nap.edu/catalog/11970

16. Basu A, Dydowiczová A, Trosko JE, Bláha L, Babica P. Ready to go 3D? A Semi-Automated Protocol for Microwell Spheroid Arrays to Increase Scalability and Throughput of 3D Cell Culture Testing. Toxicol Mech Methods. 2020; 30: 590-604. doi: 10.1080/15376516.2020.1800881.

17. Sun H, Liu G-T. Chemopreventive Effect of Bicyclol on Malignant Transformation of WB-F344 Rat Liver Epithelial Cells and its Effect on Related Signal Transduction *In Vitro*. Cancer Lett. 2006; 236: 239–49. doi: 10.1016/j.canlet.2005.05.019.

18. Elje E, Hesler M, Rundén-Pran E, Mann P, Mariussen E, Wagner S, *et al*. The Comet Assay Applied to HepG2 Liver Spheroids. Mutat Res Toxicol Environ Mutagen. 2019; 845: 403033. doi: 10.1016/j.mrgentox.2019.03.006.

19. Creton S, Aardema MJ, Carmichael PL, Harvey JS, Martin FL, Newbold RF, *et al*. Cell Transformation Assays for Prediction of Carcinogenic Potential: State of The Science and Future Research Needs. Mutagenesis. 2012; 27: 93–101. doi: 10.1093/mutage/ger053.

20. Štampar M, Breznik B, Filipič M, Žegura B. Characterization of In Vitro 3D Cell Model Developed from Human Hepatocellular Carcinoma (HepG2) Cell Line. Cells. 2020; 9: 2557. doi: 10.3390/cells9122557.

21. Štampar M. Hepatocellular Carcinoma (HepG2/C3A) Cell-Based 3D Model for Genotoxicity Testing of Chemicals. Sci Total Environ. 2021;12. doi: 10.1016/j.scitotenv.2020.143255.

22. Gheibi P, Son KJ, Stybayeva G, Revzin A. Harnessing Endogenous Signals from Hepatocytes Using a Low Volume Multi-Well Plate. Integr Biol. 2017; 9: 427–35. doi: 10.1039/c7ib00010c.

23. Hoarau-Véchot J, Rafii A, Touboul C, Pasquier J. Halfway between 2D and Animal Models: Are 3D Cultures the Ideal Tool to Study Cancer-Microenvironment Interactions? Int J Mol Sci. 2018; 19: 181. doi: 10.3390/ijms19010181.

24. Jackson EL, Lu H. Three-Dimensional Models for Studying Development and Disease: Moving on From Organisms to Organs-On-A-Chip and Organoids. Integr Biol. 2016; 8: 672–83. doi: 10.1039/c6ib00039h.

25. Duval K, Grover H, Han L-H, Mou Y, Pegoraro AF, Fredberg J, *et al*. Modeling Physiological Events in 2D vs. 3D Cell Culture. Physiology. 2017; 32: 266–77. doi: 10.1152/physiol.00036.2016.

26. Langhans SA. Three-Dimensional in Vitro Cell Culture Models in Drug Discovery and Drug Repositioning. Front Pharmacol. 2018; 9: 6. doi: 10.3389/fphar.2018.00006.

27. Pampaloni F, Stelzer E, Masotti A. Three-Dimensional Tissue Models for Drug Discovery and Toxicology. Recent Pat Biotechnol. 2009; 3: 103–17. doi: 10.2174/187220809788700201.

28. Cui X, Hartanto Y, Zhang H. Advances in Multicellular Spheroids Formation. J R Soc Interface. 2017; 14: 20160877. doi: 10.1098/rsif.2016.0877.

29. Friedrich J, Seidel C, Ebner R, Kunz-Schughart LA. Spheroid-Based Drug Screen: Considerations and Practical Approach. Nat Protoc. 2009; 4: 309-24. doi: 10.1038/nprot.2008.226.

30. Cox CR, Lynch S, Goldring C, Sharma P. Current Perspective: 3D Spheroid Models Utilizing Human-Based Cells for Investigating Metabolism-Dependent Drug-Induced Liver Injury. Front Med Technol. 2020; 2: 611913. doi: 10.3389/fmedt.2020.611913.

31. Napolitano AP, Dean DM, Man AJ, Youssef J, Ho DN, Rago AP, *et al*. Scaffold-Free Three-Dimensional Cell Culture Utilizing Micromolded Nonadhesive Hydrogels. BioTechniques. 2007; 43: 494–500. doi: 10.2144/000112591.

32. Vekemans K, Braet F. Structural and Functional Aspects of the Liver and Liver Sinusoidal Cells in Relation to Colon Carcinoma Metastasis. World J Gastroenterol. 2005; 11: 5095-102. doi: 10.3748/wjg.v11.i33.5095.

33. Zeilinger K, Freyer N, Damm G, Seehofer D, Knöspel F. Cell Sources for I*n Vitro* Human Liver Cell Culture Models. Exp Biol Med. 2016; 241: 1684–98. doi: 10.1177/1535370216657448.

34. Chang C-C, Hsu Y-H, Chou H-C, Lee Y-CG, Juan S-H. 3-Methylcholanthrene/Aryl-Hydrocarbon Receptor-Mediated Hypertension Through eNOS Inactivation. J Cell Physiol. 2017; 232: 1020–9. doi: 10.1002/jcp.25497.

35. Radaszkiewicz KA, Beckerová D, Woloszczuková L, Radaszkiewicz TW, Lesáková P, Blanářová OV, *et al.* 12-O-Tetradecanoylphorbol-13-acetate Increases Cardiomyogenesis Through PKC/ERK Signaling. Sci Rep. 2020; 10: 15922. doi: 10.1038/s41598-020-73074-4.

36. Lee H-W, Ahn D-H, Crawley SC, Li J-D, Gum JR, Basbaum CB, *et al*. Phorbol 12-Myristate 13-Acetate Up-regulates the Transcription of MUC2Intestinal Mucin via Ras, ERK, and NF-κB. J Biol Chem. 2002; 277: 32624–31. doi: 10.1074/jbc.M200353200.

37. Schindelin J, Arganda-Carreras I, Frise E, Kaynig V, Longair M, Pietzsch T, *et al*. Fiji: An Open-Source Platform for Biological-Image Analysis. Nat Methods. 2012; 9: 676–82. doi: 10.1038/nmeth.2019.

38. Schneider CA, Rasband WS, Eliceiri KW. NIH Image to ImageJ: 25 Years of Image Analysis. Nat Methods. 2012; 9: 671–5. doi: 10.1038/nmeth.2089.

39. Olson E. Particle Shape Factors and their Use in Image Analysis – Part 1: Theory. Journal of GXP Compliance. 2011, 15: 85.

40. ImageJ. ImageJ; Image Procesing and Analysis in Java. 2021. Available from: https://imagej.nih.gov/ij/docs/menus/analyze.html

41. Gawenda T, Krawczykowski D, Krawczykowska A, Saramak A, Nad A. Application of Dynamic Analysis Methods into Assessment of Geometric Properties of Chalcedonite Aggregates Obtained by Means of Gravitational Upgrading Operations. Minerals. 2020; 10: 180. doi: 10.3390/min10020180

42. Maire M-A, Pant K, Phrakonkham P, Poth A, Schwind K-R, Rast C, *et al*. Recommended Protocol for the Syrian Embryo (SHE) Cell Transformation Assay. Mutat Res Toxicol Environ Mutagen. 2012; 744: 76–81. doi: 10.1016/j.mrgentox.2011.12.010.

43. Ramaiahgari SC, den Braver MW, Herpers B, Terpstra V, Commandeur JNM, van de Water B, *et al*. A 3D *In Vitro* Model of Differentiated HepG2 Cell Spheroids with Improved Liver-Like Properties for Repeated Dose High-Throughput Toxicity Studies. Arch Toxicol. 202; Available from: http://link.springer.com/10.1007/s00204-014-1215-9